Chiral critical behavior in two dimensions from five-loop renormalization-group expansions

P. Calabrese[1], E. V. Orlov[2], P. Parruccini[3], and A. I. Sokolov[2],

[1] *Scuola Normale Superiore and INFN, Piazza dei Cavalieri 7, I-56126 Pisa, Italy.*

[2] *Department of Physical Electronics, Saint Petersburg Electrotechnical University, Professor Popov Street 5, St. Petersburg 197376, Russia.*

[3] *Dipartimento di Fisica dell' Università di Pisa and INFN, Via Buonarroti 2, I-56100 Pisa, Italy.*

e-mail: calabres@df.unipi.it, orlov@mail.lanck.net, parrucci@df.unipi.it, ais@sokol.usr.etu.spb.ru.

(February 1, 2008)

Abstract

We analyze the critical behavior of two-dimensional N-vector spin systems with noncollinear order within the five-loop renormalization-group approximation. The structure of the RG flow is studied for different N leading to the conclusion that the chiral fixed point governing the critical behavior of physical systems with $N = 2$ and $N = 3$ does not coincide with that given by the $1/N$ expansion. We show that the stable chiral fixed point for $N \leq N^*$, including $N = 2$ and $N = 3$, turns out to be a focus. We give a complete characterization of the critical behavior controlled by this fixed point, also evaluating the subleading crossover exponents. The spiral-like approach of the chiral fixed point is argued to give rise to unusual crossover and near-critical regimes that may imitate varying critical exponents seen in numerous physical and computer experiments.

I. INTRODUCTION

The critical behavior of two-dimensional frustrated spin models with noncollinear or canted order has been the object of intensive theoretical and experimental studies, being of prime interest for those investigating layered magnetic systems with special structures and superconducting Josephson-junction arrays in an external magnetic field.

In physical magnets, frustration (leading to noncollinear order) may arise either because of the special geometry of the lattice or from the competition of different kinds of interactions. An example of the first kind is the two-dimensional triangular antiferromagnet, whereas for the latter case typical models are the fully frustrated XY model on a square lattice and models with different nearest-neighbor and next-nearest-neighbor interactions. In these systems the Hamiltonian is minimized by the noncollinear configurations with a 120^o spin structure. As a consequence, at criticality, there is a breakdown of O(N) symmetry in the high-temperature phase to O($N-2$) symmetry in the ordered phase.

Field-theoretical (FT) studies of systems with noncollinear order are based on the O(N)×O(M) symmetric Landau-Ginzburg-Wilson (LGW) Hamiltonian [1–3]

$$\mathcal{H} = \int d^d x \left\{ \frac{1}{2} \sum_a \left[(\partial_\mu \phi_a)^2 + r \phi_a^2 \right] + \frac{1}{4!} u_0 \left(\sum_a \phi_a^2 \right)^2 + \frac{1}{4!} v_0 \sum_{a,b} \left[(\phi_a \cdot \phi_b)^2 - \phi_a^2 \phi_b^2 \right] \right\}, \qquad (1)$$

where ϕ_a ($1 \le a \le M$) are M sets of N-component vectors. We will consider the case $M = 2$, that, for $v_0 > 0$, describes frustrated systems with noncollinear ordering. Negative values of v_0 correspond to simple ferromagnetic or antiferromagnetic ordering, and to magnets with sinusoidal spin structures [2].

The physically relevant cases are described by the Hamiltonian (1) with $N = 2$ (frustrated XY model) and $N = 3$ (frustrated Heisenberg model). Despite the very intensive theoretical and experimental efforts to fully understand the critical behavior of these models, the situation is still controversial. For the frustrated XY model the strongly debated point is either the single critical temperature T_c exists at which both the $SO(2)$ and the Z_2 symmetries are simultaneously broken or there are two successive phase transitions at different critical temperatures. In the latter case, the order at which two phase transitions occur and the numerical values of the critical exponents are doubtful too. Obviously, studying the Hamiltonian (1), we cannot clarify the point just mentioned, since this Hamiltonian describes only the chiral phase transition. In more detail, these and other relevant issues are reviewed in Ref. [4], where one can find a complete list of references; we mention here only the very recent studies [5–8] (not quoted in Ref. [4]).

The critical behavior of the frustrated Heisenberg antiferromagnet in two dimensions is clearer: it undergoes one phase transition mediated by Z_2 topological defects. Again, a complete list of references can be found in Ref. [4]. Here the debated point concerns whether the LGW Hamiltonian is able to keep the non trivial topological excitations present in this model, to the contrary of other approaches like the nonlinear σ model ($NL\sigma$). In Ref. [4] it is claimed that it may be the case and we will assume it in the following.

The LGW Hamiltonian (1) has been extensively studied in the framework of $\epsilon = 4 - d$ [2,9,10], and by means of the $1/N$ [2,10] expansion. The existence and the stability properties of the fixed points were found to depend on N and on the spatial dimensionality [2,3]. Within

the ϵ expansion, for sufficiently large values of N the renormalization group equations possess four fixed points: the Gaussian fixed point ($v = u = 0$), the $O(2N)$ ($v = 0$) one and two anisotropic fixed points located in the region $u, v > 0$ and usually named chiral and antichiral. The chiral fixed point is the only stable one. There is a critical dimensionality N_c where the chiral and antichiral fixed points coalesce and disappear for $N < N_c$. In the last case, under the absence of any stable fixed point the system undergoes a weak first-order phase transition, since the associated RG flows run away from the region of stability of the fourth-order form in the free energy expansion. The three-loop estimate of N_c is [9]

$$N_c = 21.8 - 23.4\epsilon + 7.1\epsilon^2 + O(\epsilon^3)\,, \tag{2}$$

that, after an appropriate resummation, results in $N_c > 3$ in three dimensions. This inequality leads to the conclusion that for the physical models with $N = 2, 3$ the three-dimensional chiral transition is first order, as corroborated also by some other RG studies [11,12]. To the contrary, both for $N = 2$ and $N = 3$ the highest-order six-loop calculations in three dimensions [13] reveal a strong evidence for a stable chiral fixed point that, however, is not related to its counterpart found within the ϵ expansion. The four-loop two-dimensional analysis shows an equivalent topology of the fixed points location in the renormalized coupling constants plane [4]. Furthermore, in a recent work [14] we claimed that both in two and three dimensions the controversial situation may reflect the quite unusual mode of critical behavior of the N-vector chiral model under the physical values of N. It was shown that this critical behavior is governed by a stable fixed point which is a focus, attracting RG trajectories in a spiral-like manner. Approaching the fixed point in a nonmonotonic way, looking somewhat irregular, may result in a large variety of the crossover and near-critical regimes.

In this paper, we report the perturbative five-loop two-dimensional RG expansions and carry out their analysis. Some of the results for $N = 2$ and $N = 3$ was already anticipated in [14]. We point out the idea that the critical behavior for large N is the one predicted by the ϵ expansion. With decreasing N, the stable chiral fixed point becomes focuslike at some marginal value of N, N^* that differs, in principle, from N_c where both chiral and antichiral fixed points disappear. With the precision of our calculations, we are not able to fully clarify if there is a region of values of N, where the chiral transition is first order. It is worthy to note that the parallel work on the three-dimensional models [15] reveals a full analogy between chiral critical behaviors in two and three dimensions.

The paper is organized as follows. In Sec. II we derive the perturbative series for the renormalization-group functions up to five-loop order. The resummations methods and the results of the analysis are presented in Sec. III. In Sec. IV we draw our conclusions.

II. PERTURBATIVE EXPANSIONS IN TWO DIMENSIONS

A. Renormalization of the theory

The fixed-dimension field-theoretical approach [16] represents an effective procedure in the study of the critical properties of systems that undergo second-order phase transitions [17]. In the case under consideration, the expansion is performed in two quartic coupling

constants of the Hamiltonian (1). The theory is renormalized by a set of zero-momentum conditions for the one-particle irreducible two-point correlation function, four-point correlation function, and two-point correlation function with an insertion of the operator $\frac{1}{2}\phi^2$:

$$\Gamma^{(2)}_{ai,bj}(p) = \delta_{a,b}\delta_{i,j} Z_\phi^{-1} \left[m^2 + p^2 + O(p^4) \right], \tag{3}$$

$$\Gamma^{(4)}_{abcd}(0) = Z_\phi^{-2} m \left[\frac{u}{3} \left(\delta_{ab}\delta_{cd} + \delta_{ac}\delta_{bd} + \delta_{ad}\delta_{bc} \right) + v\, C_{ai,bj,ck,dl} \right], \tag{4}$$

$$\Gamma^{(1,2)}_{ab}(0) = \delta_{ab} Z_t^{-1}, \tag{5}$$

where $C_{ai,bj,ck,dl}$ is an appropriate combinatorial factor [4,13].

The perturbative knowledge of the functions $\Gamma^{(2)}$, $\Gamma^{(4)}$, and $\Gamma^{(1,2)}$ allows one to relate the renormalized physical parameters (u, v, m) to the bare ones $(u_0, v_0, r\ )$.

The fixed points of the model are defined by the common zeros of the β functions,

$$\beta_u(u,v) = m \left. \frac{\partial u}{\partial m} \right|_{u_0,v_0}, \quad \beta_v(u,v) = m \left. \frac{\partial v}{\partial m} \right|_{u_0,v_0}. \tag{6}$$

The stability properties of these points are determined by the eigenvalues ω_i of the matrix:

$$\Omega = \begin{pmatrix} \dfrac{\partial \beta_u(u,v)}{\partial u} & \dfrac{\partial \beta_u(u,v)}{\partial v} \\ \dfrac{\partial \beta_v(u,v)}{\partial u} & \dfrac{\partial \beta_v(u,v)}{\partial v} \end{pmatrix}. \tag{7}$$

A fixed point is stable if both the eigenvalues have a positive real part. If the eigenvalues possess nonvanishing imaginary parts, the fixed point is called a focus and the corresponding RG trajectories are spirals. The eigenvalues ω_i are connected to the leading scaling corrections, which go as $\xi^{-\omega_i} \sim |t|^{\Delta_i} = |t|^{\nu\omega_i}$, with few exceptions as the two-dimensional Ising model (see for a discussion Ref. [18]).

The values of the critical exponents η, ν and γ are related to the RG functions η_ϕ and η_t evaluated at the stable fixed point:

$$\eta = \eta_\phi(u^*, v^*), \tag{8}$$

$$\nu = \left[2 - \eta_\phi(u^*, v^*) + \eta_t(u^*, v^*) \right]^{-1}, \tag{9}$$

where

$$\eta_\phi(u,v) = \left. \frac{\partial \ln Z_\phi}{\partial \ln m} \right|_{u_0,v_0} = \beta_u \frac{\partial \ln Z_\phi}{\partial u} + \beta_v \frac{\partial \ln Z_\phi}{\partial v}, \tag{10}$$

$$\eta_t(u,v) = \left. \frac{\partial \ln Z_t}{\partial \ln m} \right|_{u_0,v_0} = \beta_u \frac{\partial \ln Z_t}{\partial u} + \beta_v \frac{\partial \ln Z_t}{\partial v}. \tag{11}$$

B. Five-loop series

In this section we extend the four-loop perturbative series [4] for the RG functions β_u, β_v, η_ϕ, and η_t up to five-loop order using the numerical values of two-dimensional five-loop integrals evaluated in Ref. [19].

In order to obtain finite fixed point values in the limit of infinite components of the order parameter ($N \to \infty$) we use the rescaled couplings

$$u \equiv \frac{8\pi}{3}\, R_{2N}\, \overline{u}, \qquad\qquad v \equiv \frac{8\pi}{3}\, R_{2N}\, \overline{v}, \tag{12}$$

where $R_N = 9/(8+N)$.

The resulting RG series are [20]:

$$\bar\beta_{\overline{u}} = -\overline{u} + \overline{u}^2 + \frac{1-N}{(4+N)}\bar u\bar v - \frac{1-N}{(8+2N)}\overline{v}^2 + \sum_{i+j\geq 3} b_{ij}^{(u)} \overline{u}^i \overline{v}^j, \tag{13}$$

$$\bar\beta_{\overline{v}} = -\overline{v} - \frac{1}{2}\frac{6-N}{(4+N)}\overline{v}^2 + \frac{6}{(4+N)}\bar u\bar v + \sum_{i+j\geq 3} b_{ij}^{(v)} \overline{u}^i \overline{v}^j, \tag{14}$$

$$\eta_\phi = \frac{1.83417\,(1+N)}{(8+2N)^2}\overline{u}^2 + \frac{1.83417\,(1-N)}{(8+2N)^2}\bar u\bar v - \frac{1.37563\,(1-N)}{(8+2N)^2}\overline{v}^2 + \sum_{i+j\geq 3} e_{ij}^{(\phi)} \overline{u}^i \overline{v}^j, \tag{15}$$

$$\begin{aligned}\eta_t = &-\frac{2\,(1+N)}{(4+N)}\overline{u} - \frac{(1-N)}{(4+N)}\overline{v} + \frac{13.5025\,(1+N)}{(8+2N)^2}\overline{u}^2 + \frac{13.5025\,(1-N)}{(8+2N)^2}\bar u\bar v \\ &-\frac{10.1269\,(1-N)}{(8+2N)^2}\overline{v}^2 + \sum_{i+j\geq 3} e_{ij}^{(t)} \overline{u}^i \overline{v}^j,\end{aligned} \tag{16}$$

where

$$\bar\beta_{\overline{u}} = \frac{3}{16\pi}\, R_{2N}^{-1}\beta_u, \qquad\qquad \bar\beta_{\overline{v}} = \frac{3}{16\pi}\, R_{2N}^{-1}\beta_v. \tag{17}$$

Only the five-loop coefficients $b_{ij}^{(u)}$, $b_{ij}^{(v)}$, $e_{ij}^{(\phi)}$ and $e_{ij}^{(t)}$ are reported in Table I, since up to the fourth order they are reported in Ref. [4]. Note that, due to the last rescaling, the element of the Ω matrix (7) are two times the derivative of $\bar\beta$ with respect to $\overline{u}$ and $\overline{v}$.

We verify the exactness of our series by checking them in particular limits ($N = 1$, $\bar v = 0$, $N = M = 2$, $N \to \infty$) as in Ref. [4].

III. RESUMMATION AND ANALYSIS OF THE FIVE-LOOP SERIES

The field theoretical perturbative expansions are known to be divergent asymptotic series. Quantitative informations may be extracted from these series exploiting the properties of Borel summability for ϕ^4 theories in two and three dimensions and resumming them by a Borel transformation combined with a method for the analytical extension of the Borel transform. This last procedure can be realized by using Padé approximants or via a conformal mapping, which maps the domain of analyticity of the Borel transform (cut at the instanton singularity) $\overline{u}_b$ onto a circle [21].

TABLE I. Five-loop coefficients $b_{ij}^{(u)}$, $b_{ij}^{(v)}$, $e_{ij}^{(\phi)}$ and $e_{ij}^{(t)}$ of RG functions.

i,j	$R_{2N}^{-i-j} b_{ij}^{(u)}$
6,0	$+2.01674 + 2.10643\,N + 0.716897\,N^2 + 0.0887555\,N^3 + 0.00241689\,N^4 - 2.45381 * 10^{-7}\,N^5$
5,1	$+2.92727 - 1.33251\,N - 1.34924\,N^2 - 0.238028\,N^3 - 0.00748703\,N^4 - 0.000013119\,N^5$
4,2	$-4.43837 + 2.03796\,N + 2.0376\,N^2 + 0.352602\,N^3 + 0.0101649\,N^4 + 0.0000459364\,N^5$
3,3	$+3.19454 - 1.49238\,N - 1.45358\,N^2 - 0.242665\,N^3 - 0.0058521\,N^4 - 0.0000594059\,N^5$
2,4	$-1.15807 + 0.561265\,N + 0.515855\,N^2 + 0.0797969\,N^3 + 0.00112123\,N^4 + 0.0000298703\,N^5$
1,5	$+0.222479 - 0.113395\,N - 0.095816\,N^2 - 0.0132978\,N^3 + 0.0000283847\,N^4 + 1.2973 * 10^{-6}\,N^5$
0,6	$-0.0151778 + 0.00751941\,N + 0.00660415\,N^2 + 0.00104974\,N^3 + 8.90815 * 10^{-6}\,N^4 - 4.38647 * 10^{-6}\,N^5$

i,j	$R_{2N}^{-i-j} b_{ij}^{(v)}$
5,1	$+6.24588 + 3.59449\,N + 0.620789\,N^2 + 0.0264763\,N^3 - 0.000525164\,N^4 - 0.0000277103\,N^5$
4,2	$-8.7215 - 4.66521\,N - 0.686267\,N^2 - 0.0125189\,N^3 + 0.00131132\,N^4 + 0.0000937132\,N^5$
3,3	$+6.32764 + 3.38603\,N + 0.514699\,N^2 + 0.0164667\,N^3 - 0.00034289\,N^4 - 0.000120039\,N^5$
2,4	$-2.44897 - 1.35035\,N - 0.227251\,N^2 - 0.0119867\,N^3 - 0.0000336496\,N^4 + 0.0000731821\,N^5$
1,5	$+0.48559 + 0.257994\,N + 0.0396213\,N^2 + 0.000895835\,N^3 - 0.000205336\,N^4 - 0.0000218222\,N^5$
0,6	$-0.036149 - 0.0191764\,N - 0.00232213\,N^2 + 0.000377994\,N^3 + 0.0000915813\,N^4 + 2.59344 * 10^{-6}\,N^5$

i,j	$R_{2N}^{-i-j} e_{ij}^{(\phi)}$
5,0	$-0.00722954 - 0.011019\,N - 0.00391279\,N^2 - 0.000142581\,N^3 - 0.0000192165\,N^4$
4,1	$-0.0180738 + 0.00860027\,N + 0.00916515\,N^2 + 0.00026037\,N^3 + 0.0000480413\,N^4$
3,2	$+0.0260483 - 0.0129479\,N - 0.0129842\,N^2 - 0.0000681925\,N^3 - 0.0000480413\,N^4$
2,3	$-0.0161648 + 0.00849874\,N + 0.00785318\,N^2 - 0.000211121\,N^3 + 0.0000240207\,N^4$
1,4	$+0.00411472 - 0.00235806\,N - 0.00191523\,N^2 + 0.000164576\,N^3 - 6.00516 * 10^{-6}\,N^4$
0,5	$-0.000397627 + 0.000247705\,N + 0.000181639\,N^2 - 0.0000311162\,N^3 - 6.00516 * 10^{-7}\,N^4$

i,j	$R_{2N}^{-i-j} e_{ij}^{(t)}$
5,0	$-0.285954 - 0.463731\,N - 0.195487\,N^2 - 0.0176704\,N^3 + 0.000039754\,N^4$
4,1	$-0.714885 + 0.270442\,N + 0.400167\,N^2 + 0.0443747\,N^3 - 0.000099385\,N^4$
3,2	$+0.954626 - 0.384666\,N - 0.520913\,N^2 - 0.0491461\,N^3 + 0.0000993852\,N^4$
2,3	$-0.572386 + 0.253092\,N + 0.29846\,N^2 + 0.0208835\,N^3 - 0.0000496928\,N^4$
1,4	$+0.149502 - 0.0775891\,N - 0.0701865\,N^2 - 0.00179722\,N^3 + 0.0000708398\,N^4$
0,5	$-0.0157319 + 0.0101789\,N + 0.00583765\,N^2 - 0.00022754\,N^3 - 0.0000571742\,N^4$

Let us consider a perturbative series in $\overline{u}$ and $\overline{v}$

$$R(\overline{u},\overline{v}) = \sum_{k=0}^{l} \sum_{h=0}^{l-k} R_{hk} \overline{u}^h \overline{v}^k, \tag{18}$$

which we want to resum (i.e., one of the η or β functions). In the Padé-Borel method we use the trick of the resolvent series considering the Borel transformed function,

$$\tilde{R}(\lambda,\overline{u},\overline{v},b) = \sum_{n=0}^{\infty} \frac{\lambda^n}{\Gamma(n+b+1)} \sum_{l=0}^{n} R_{l,n-l} \overline{u}^l \overline{v}^{n-l}. \tag{19}$$

Calling $P_M^N(\lambda,\overline{u},\overline{v},b)$ the $[N/M]$ Padé approximant of the series $\tilde{R}(\lambda,\overline{u},\overline{v},b)$ in the variable λ, one obtains the estimate of the desired quantity as

$$\tilde{P}_M^N(b,\overline{u},\overline{v}) = \int_0^{\infty} e^{-t} t^b P_M^N(t,\overline{u},\overline{v},b) dt. \tag{20}$$

In this way we produce several approximants of the function $R(\overline{u},\overline{v})$ with varying the parameters b, N, and M.

In the conformal mapping method, the idea is to exploit, in the course of the resummation, the knowledge of the large order behavior of the series $R(\overline{u},\overline{v})$ at fixed $z = \overline{v}/\overline{u}$ [22,13,4]. This large-order behavior is related to the singularity of the Borel transform closest to the

origin [23]. For the Hamiltonian (1), the value of the Borel transform singularity closest to the origin $\overline{u}_b$ has been computed in Ref [4], obtaining:

$$\begin{aligned} \frac{1}{\overline{u}_b} &= -\,a\,R_{2N} \qquad\qquad \text{for} \qquad 0 < z < 4, \\ \frac{1}{\overline{u}_b} &= -\,a\,R_{2N}\,\left(1 - \frac{1}{2}z\right) \qquad \text{for} \qquad z < 0, \quad z > 4, \end{aligned} \tag{21}$$

where $a = 0.238659217\ldots$. For $z > 2$ there is a singularity on the real positive axis which, however, is not the closest one to the origin for $z < 4$. Thus, for $z > 2$ the series are not Borel summable. We resum the RG functions also for the values of z for which the series are not Borel summable since the method should provide a reasonable estimate if $z < 4$, because we take into account the leading large-order behavior.

With the knowledge of $\overline{u}_b$, one can perform the mapping

$$y(\overline{u}; z) = \frac{\sqrt{1 - \overline{u}/\overline{u}_b(z)} - 1}{\sqrt{1 - \overline{u}/\overline{u}_b(z)} + 1}, \tag{22}$$

in order to extend $R(\overline{u}, \overline{u}z)$ to all positive values of $\overline{u}$. Consequently one obtains the set of approximants

$$E(R)_p(\alpha, b; \overline{u}, \overline{v}) = \sum_{k=0}^{p} B_k(\alpha, b; \overline{v}/\overline{u}) \times \int_0^\infty dt\, t^b e^{-t} \frac{y(\overline{u}t; \overline{v}/\overline{u})^k}{[1 - y(\overline{u}t; \overline{v}/\overline{u})]^\alpha}, \tag{23}$$

where the coefficient B_k is determined by the condition that the expansion of $E(R)_p(\alpha, b; \overline{u}, \overline{v})$ in powers of $\overline{u}$ and $\overline{v}$ gives $R(\overline{u}, \overline{v})$ to order p.

An important issue in the fixed dimension approach to critical phenomena concerns the analytic properties of the β functions. As shown in Ref. [18] for the $O(N)$ model, the presence of confluent singularities in the zero of the perturbative β function causes a slow convergence of the resummation of the perturbative series to the correct fixed-point value. The apparent stability of the results when analyzing a finite number of terms of the perturbative expansion may not provide a reliable indication of the uncertainty of the overall estimates. The $O(N)$ two-dimensional field-theory valuations of physical quantities [21,19] are less accurate than the three-dimensional counterparts, due to the bigger critical value of the quartic coupling constant and stronger nonanalyticities at the fixed point [18,24,25]. In Ref. [18] it is explicitly shown that the nonanalytic terms cause a large deviation in the estimate of the right correction to the scaling, i.e., the exponent ω. At the same time, the perturbative results for the fixed-point location turn out to be rather good approximations for the exact ones. We think that a similar situation holds for frustrated models.

A. Fixed points, stability, and critical exponents

In order to calculate the fixed points of the theory, we resum the perturbative expression for each β function in the whole plane $(\overline{u}, \overline{v})$ following the procedure explained above. With the conformal mapping method, we choose the approximants that stabilize the series for

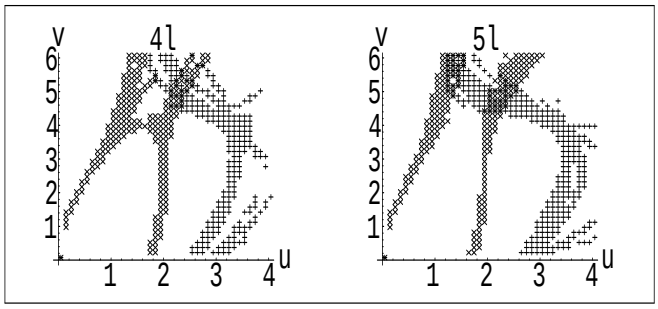

FIG. 1. Zeros of $\bar{\beta}$ functions for $N = 2$ in the $(\overline{u}, \overline{v})$ plane. Pluses (+) and crosses (×) correspond to zeroes of $\bar{\beta}_{\overline{v}}(\overline{u}, \overline{v})$ and $\bar{\beta}_{\overline{u}}(\overline{u}, \overline{v})$, respectively.

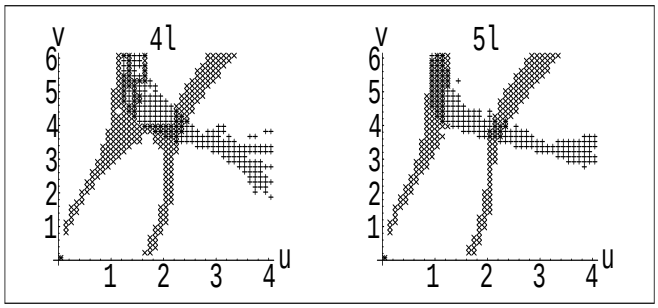

FIG. 2. Zeros of $\bar{\beta}$ functions for $N = 3$ in the $(\overline{u}, \overline{v})$ plane. Pluses (+) and crosses (×) correspond to zeroes of $\bar{\beta}_{\overline{v}}(\overline{u}, \overline{v})$ and $\bar{\beta}_{\overline{u}}(\overline{u}, \overline{v})$, respectively.

small values of the coupling constants with varying the considered perturbative order, i.e., $\alpha = 0, 1, 2$ and $b = 5, 7, \ldots, 15$. In this manner we have 18 approximants for each $\bar{\beta}$ function. To obtain reasonable values and error bars for the fixed-point coordinates, we divide the domain $0 \leq \overline{u} \leq 4$, $0 \leq \overline{v} \leq 6$ in 40^2 rectangles, and we mark all the sites in which at least two approximants for $\bar{\beta}_{\overline{u}}$ and $\bar{\beta}_{\overline{v}}$ vanish. This procedure is applied for the four-loop and five-loop series and the results for the zeros of the β functions for $N = 2$ and $N = 3$ are displayed in Figs. 1 and 2, respectively. We remind the reader that the four-loop results were previously reported in Ref. [4], where similar figures were shown also for the three-loop case. It was also shown that no upper branch of zeros of $\bar{\beta}_{\overline{u}}$ appears in the three-loop approximation for all considered values of N.

As one can see from Figs. 1 and 2, for these physical systems the resummed RG expansions yield similar pictures for the zeros of the $\bar{\beta}$ functions. The existence of three fixed points – the gaussian, the $O(2N)$, and the chiral – is clear in both cases, while the presence of an unstable antichiral fixed point looks doubtful. In fact, if this last point exists, it should be located in the domain where the resummation procedure fails to give reliable quantitative results ($z > 4$).

The location of the chiral fixed point for $N = 2$ is

$$[u^*, v^*] = \quad [2.3(2), 5.0(5)] \qquad \text{(4-loop CM)}, \tag{24}$$

$$[2.25(25), 4.80(45)] \qquad \text{(5-loop CM)}, \tag{25}$$

$$[2.35(30), 4.35(25)] \qquad \text{(Padé)}, \tag{26}$$

and for $N = 3$

$$[u^*, v^*] = \quad [2.3(3), 3.9(5)] \qquad \text{(4-loop CM)}, \tag{27}$$
$$[2.2(2), 3.9(3)] \qquad \text{(5-loop CM)}, \tag{28}$$
$$[2.25(20), 3.60(15)] \qquad \text{(Padé)}. \tag{29}$$

The stability properties of the chiral fixed point depend on the signs of the real parts of the eigenvalues ω_i of the Ω matrix. We take the above 18 approximants for each $\bar{\beta}$ function and compute the numerical derivatives of each couple of approximants of the two $\bar{\beta}$ functions at their common zero, obtaining 324 possible combinations. To have reliable numerical estimates for ω_i, we limit ourselves by the approximants that yield the chiral fixed point coordinates compatible with their final, properly weighted values.

Both for $N = 2$ and $N = 3$, we find that the chiral fixed point is a stable focus since it possesses stability eigenvalues with nonvanishing imaginary parts and positive real parts. At the five-loop (four-loop) approximations for $N = 2$ the complex eigenvalues are produced by 87% (87%) of the working approximants within the conformal mapping method, while for $N = 3$ by 89% (74%) of the approximants employed. When estimating the averaged eigenvalues of the Ω matrix at the chiral fixed point, we disregard the approximants leading to purely real eigenvalues. For $N = 2$ the final results of our calculations are:

$$\omega_\pm = 1.50(25) \pm i\, 1.00(45), \quad \text{(4-loop CM)} \tag{30}$$
$$\omega_\pm = 2.05(35) \pm i\, 0.80(55), \quad \text{(5-loop CM)} \tag{31}$$

and for $N = 3$

$$\omega_\pm = 1.30(25) \pm i\, 0.50(35), \quad \text{(4-loop CM)} \tag{32}$$
$$\omega_\pm = 1.55(25) \pm i\, 0.55(35), \quad \text{(5-loop CM)} \tag{33}$$

The presence of imaginary parts comparable in magnitude with the real ones leads to the conclusion that the critical behaviors of frustrated two-dimensional Heisenberg and XY

TABLE II. Location of the chiral fixed point with its stability eigenvalues, critical exponent η, and crossover exponent $\omega_{O(2N)}$ at the $O(2N)$ fixed point.

$N = 2$	Padé	C.M. (4 loop)	C.M. (5 loop)
$\overline{u}^*$	2.35(30)	2.3(2)	2.25(25)
$\overline{v}^*$	4.35(25)	5.0(5)	4.80(45)
$\omega_\pm$	$2.33(65) \pm i0.62(48)$	$1.50(25) \pm i1.00(45)$	$2.05(35) \pm i0.80(55)$
η	0.3(1)	0.29(5)	0.28(8)
$\omega_{O(4)}$		-0.36(4)	-0.35(16)
$N = 3$	Padé	C.M.(4 loop)	C.M.(5 loop)
$\overline{u}^*$	2.25(20)	2.3(3)	2.2(2)
$\overline{v}^*$	3.60(15)	3.9(5)	3.9(3)
$\omega_\pm$	$1.77(43) \pm i0.47(18)$	$1.30(25) \pm i0.50(35)$	$1.55(25) \pm i0.55(35)$
η	0.23(7)	0.24(6)	0.23(5)
$\omega_{O(6)}$		-0.7(2)	-0.69(9)

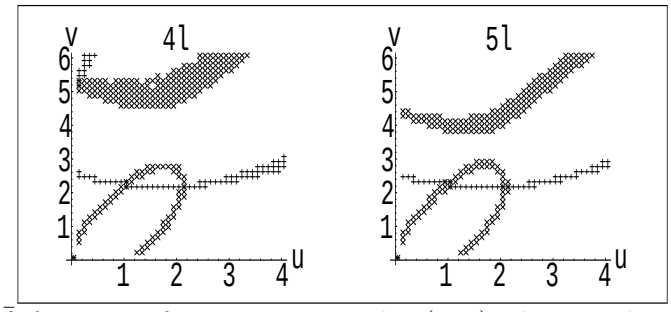

FIG. 3. Zeros of $\bar{\beta}$ functions for $N = 32$ in the $(\overline{u}, \overline{v})$ plane. Pluses (+) and crosses (×) correspond to zeroes of $\bar{\beta}_{\overline{v}}(\overline{u}, \overline{v})$ and $\bar{\beta}_{\overline{u}}(\overline{u}, \overline{v})$, respectively.

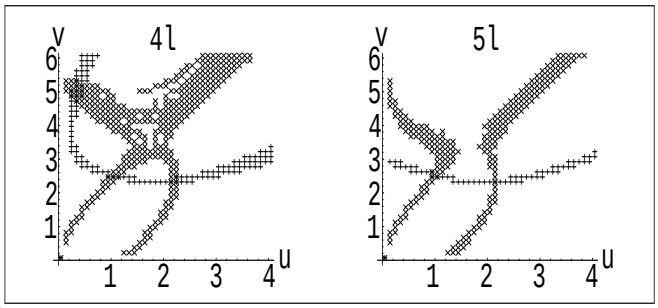

FIG. 4. Zeros of $\bar{\beta}$ functions for $N = 16$ in the $(\overline{u}, \overline{v})$ plane. Pluses (+) and crosses (×) correspond to zeroes of $\bar{\beta}_{\overline{v}}(\overline{u}, \overline{v})$ and $\bar{\beta}_{\overline{u}}(\overline{u}, \overline{v})$, respectively.

systems are driven by focus fixed points. To strengthen this new and important issue, we repeat the analysis of the stability properties of the chiral fixed point by a Padé study, which confirms the previous results, although the statistics in this case is much less significant due to a large number of defective Padé approximants. All the results obtained are summarized in Table II. Note that in the past such a behavior was found in three dimensions within the three-loop RG approximation but only for unphysical values of N ($N = 5, 6, 7$) [27].

In order to fully characterize the two physical systems discussed, we calculate the critical exponents as well. For the exponent η we find values that agree with the results of the four-loop analysis [4]. At the same time, we can not give a reasonable estimate for the critical exponent ν because of the strong oscillations observed with varying the working approximants.

Finally, we report in Table II the five-loop estimate of the crossover exponent $\omega_{O(2N)}$, finding that the Heisenberg fixed point is unstable for both $N = 2, 3$, in agreement with the previous four-loop calculation [4].

We apply the same kind of analysis also to the models with $N \geq 4$. All these systems are free of topological defects [4] and are well described by appropriate $NL\sigma$ models [26] which provide the existence of a stable chiral fixed point with critical exponents and corrections to the scaling equal to the ones of a system with an infinite number of components of the order parameter.

The zeros of the two βs for $N = 32, 16, 8, 6, 4$ are shown in Fig. 3, 4, 5, 6, 7. From these figures it is clear that for large enough values of N four fixed points exist: the gaussian, the $O(2N)$, the chiral, and the antichiral, with a topological structure similar to the one found in ϵ expansion for $N > N_c$. The location of the chiral fixed point for various N is reported

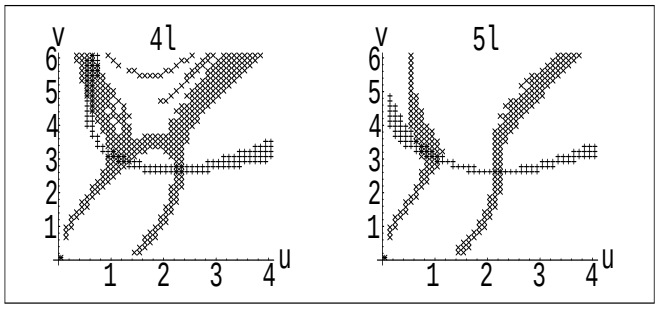

FIG. 5. Zeros of $\bar{\beta}$ functions for $N = 8$ in the $(\overline{u}, \overline{v})$ plane. Pluses (+) and crosses (×) correspond to zeroes of $\bar{\beta}_{\overline{v}}(\overline{u}, \overline{v})$ and $\bar{\beta}_{\overline{u}}(\overline{u}, \overline{v})$ respectively.

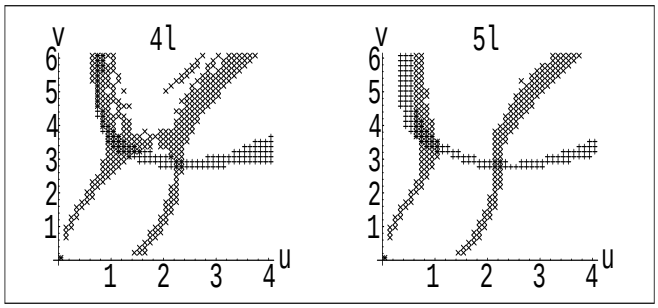

FIG. 6. Zeros of $\bar{\beta}$ functions for $N = 6$ in the $(\overline{u}, \overline{v})$ plane. Pluses (+) and crosses (×) correspond to zeroes of $\bar{\beta}_{\overline{v}}(\overline{u}, \overline{v})$ and $\bar{\beta}_{\overline{u}}(\overline{u}, \overline{v})$ respectively.

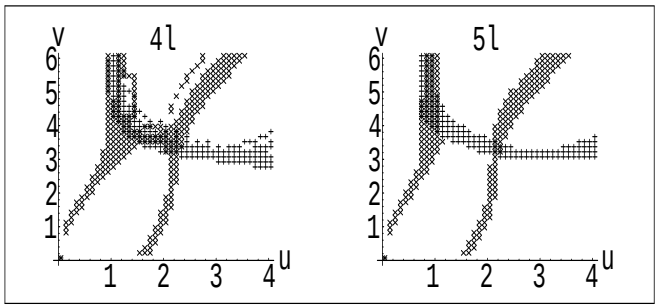

FIG. 7. Zeros of $\bar{\beta}$ functions for $N = 4$ in the $(\overline{u}, \overline{v})$ plane. Pluses (+) and crosses (×) correspond to zeroes of $\bar{\beta}_{\overline{v}}(\overline{u}, \overline{v})$ and $\bar{\beta}_{\overline{u}}(\overline{u}, \overline{v})$ respectively.

in Tab. III.

From the $NL\sigma$ model it is expected $\omega_1 = \omega_2 = 2$ [26]. For this reason N^* should be less or at least equal to 4. From our analysis we find that the chiral fixed point is stable for all the considered N. However, the estimates for ω_i are slighty different from 2, also for large N (e.g., for $N = 16$ we find $\omega_1 = 1.59(5)$ and $\omega_2 = 2.01(11)$). Such a disagreement was already observed in the four-loop approximation, and it may be attributed to the nonanalyticities discussed in the previous subsection. We observe that for $N \geq 8$ all the stability eigenvalues are purely real, but for $N = 6$ about the 50% of the five-loop approximants possess a nonvanishing imaginary part, suggesting $N^* \sim 6$. This result seems to disagree with the $NL\sigma$ prediction. Again this might be due to nonanalyticities.

To further approve the above conclusions, we apply, along with the conformal-mapping based, the resummation by means of the Padé-Borel technique. In the region where the

TABLE III. Location of the stable chiral fixed point for $N \geq 4$.

N	C.M.(4 loop)	C.M.(5 loop)	Padé
4		[2.2(1),3.37(23)]	[2.22(16),3.19(10)]
6	[2.26(7),2.85(15)]	[2.21(6),2.80(8)]	[2.25(10),2.79(4)]
8	[2.28(9),2.66(8)]	[2.22(7),2.61(6)]	[2.23(6),2.61(3)]
16	[2.22(4),2.37(3)]	[2.17(5),2.33(3)]	[2.18(2),2.33(3)]
32	[2.128(16),2.19(1)]	[2.09(2),2.16(2)]	[2.100(15),2.165(10)]

fixed point is expected, many Padé approximants turn out to be defective, i.e., possessing dangerous poles. We find that the approximants [4/1], [3/1], and [2/2] are nondefective in the majority of the cases. Considering these three Padé approximants with $b = 0, 1, 2$ (being the more stable under variation of the number of loops), we finally have nine approximants for each β function. The location of the chiral fixed point is reported in Table III, with all the defective cases discarded.

We also compute the exponents η and η_t with both the resummation techniques. We consider a lot of approximants and finally we choose the more stable ones with varying the number of loops. The found values are close to those of the $O(N)$ model for $N \geq 3$, but differ from the exact ones coming from $NL\sigma$ model $\eta = 0$ and $\eta_t = -2$ (e.g., we find $\eta_t = -1.95(20)$ for $N = 16$ and $\eta = 0.16(2)$ for $N = 6$). We think these discrepancies are due to nonanalyticities, as in the case of $O(N)$ models. To conclude the analysis of the fixed points, we study the stability of the Heisenberg fixed point by calculating the crossover exponent $\omega_{O(2N)}$. The five-loop results show that this fixed point is unstable, in agreement with the conclusion drawn earlier from the four-loop series [4].

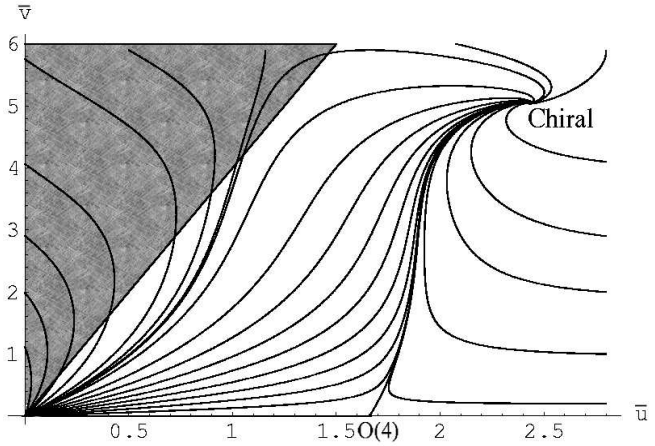

FIG. 8. RG flow for the two-dimensional chiral model with $N = 2$. The approximants used are given by $\alpha = 1$ and $b = 5$ for $\beta_{\bar{u}}$ and $\alpha = 0$ and $b = 8$ for $\beta_{\bar{v}}$. In this case, the chiral fixed point is at $(2.427, 5.045)$.

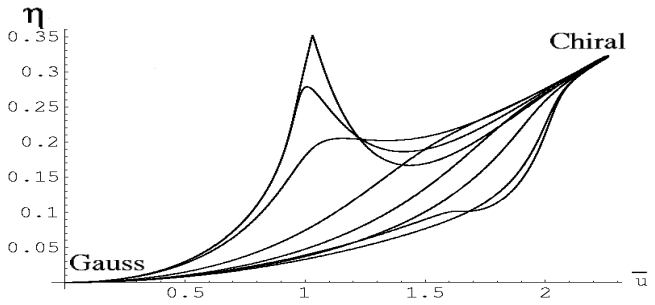

FIG. 9. Crossover of the effective exponent η_{eff} for $N = 2$.

B. Renormalization-group flow and crossover

In this subsection we demonstrate the structure of the RG flow for physical values of N. As it was already shown, a stable focus governs the critical behavior of these systems. In Fig. 8 ($N = 2$) one can see the spiral-like approach of the stable fixed point which is peculiar for the fixed points with stability eigenvalues possessing nonvanishing imaginary parts. The shaded area is the region where the resummation procedure is expected to fail (i.e., $z > 4$), since we do not take into account the singularity of the Borel transform closest to the origin that is on the real positive axis (cf. Eq (21)). Consequently, the RG trajectories given by the resummed perturbative series are quantitatively correct only within the unshaded areas. We report, nevertheless, the RG flows in other parts of the coupling constant plane in order to present a complete qualitative picture. Note, that the domain usually referred to as the sector of the first-order transitions, where the positiveness of the quartic form in the free-energy expansion breaks down, is given by the inequality $z > 2$. In fact, however, because of the presence of the higher-order terms in this expansion keeping the system globally stable at any temperature, the true domains of the first-order transitions should be more narrow.

From Fig. 8 we see that for some initial values of $(\overline{u}, \overline{v})$ the RG trajectories have the coordinate $\overline{v}$ that grows very fast at the beginning and seems to reach the region of the first-order phase transitions, but just before arriving there these trajectories drastically curve moving toward the stable chiral fixed point. These bizarre trajectories can imitate both the discontinuous phase transitions and strongly scattered effective critical exponents observed in numerous physical and computer experiments. To substantiate the former scenario, we calculate the numerical values which the effective exponent η_{eff} takes along the RG trajectories running from the Gaussian fixed point to the chiral one. Corresponding curves are shown in Fig. 9. As is seen from this figure, the exponent oscillates within a large range, even near the stable fixed point.

We demonstrate also the RG flows for $N = 3$ (Fig. 10) and for $N = 8 > N^*$ (Fig. 11). In the former (physical case) the stable fixed point is a focus and phase trajectories approach it in a spiral-like manner. In the latter (unphysical case) the stable fixed point turns out to be a node and the trajectories are certainly not spirals. Also for $N = 3$ we estimate the effective exponent η_{eff} along the RG trajectories running from the Gaussian fixed point to the chiral one. The corresponding curves (cf. Fig. 12) show big oscillations and sometimes reach negative values. We note that these negative values are obtained only in the region where the resummation is not sure, i.e., $z > 4$. Nevertheless, this strange

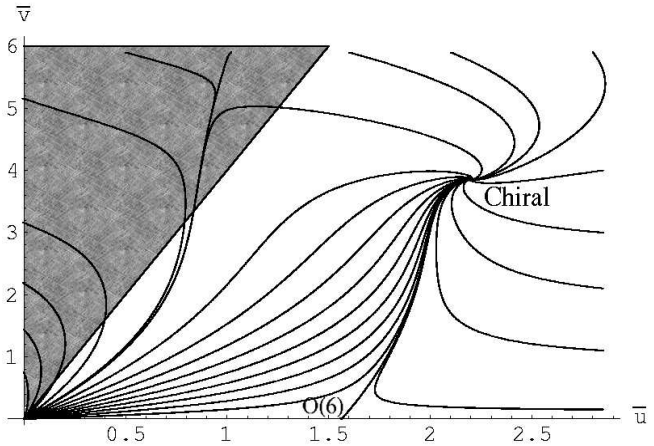

FIG. 10. RG flow for the two-dimensional chiral model with $N = 3$. Both β functions are given by approximants given by $\alpha = 2$ and $b = 9$, the chiral fixed point is located at $(1.702, 2.858)$.

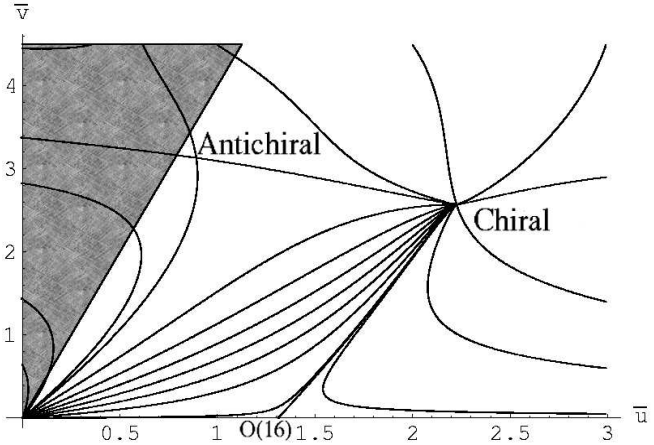

FIG. 11. RG flow for the two-dimensional model with $N = 8$. The approximants used are given by $\alpha = 0$ and $b = 7$ for $\beta_{\bar{u}}$ and $\alpha = 1$ and $b = 5$ for $\beta_{\bar{v}}$. In this case, the chiral fixed point is at $(2.226, 2.571)$ and the antichiral fixed point is at $(0.891, 3.133)$.

crossover, if reproduced from the three-dimensional series [15], might explain some doubtful experimental results, where a negative η was found.

To conclude, it is worthy to note that earlier the focuslike stable fixed points were found on the RG flow diagrams of the model describing critical behavior of liquid crystals [28] and of the $O(n)$-symmetric systems undergoing first-order phase transition close to the tricritical point [29]. In those cases, however, the independent coupling constants had different scaling dimensionality and played essentially different roles in critical thermodynamics. Moreover, recently complex subleading exponents were found from the high-temperature expansion of Dyson's hierarchical Ising model [30].

IV. CONCLUSIONS

We studied the critical thermodynamics of the two-dimensional N-vector chiral model in the five-loop RG approximation. Using the advanced resummation technique based upon

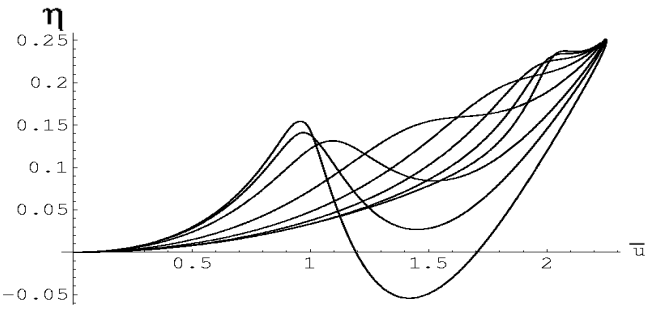

FIG. 12. Crossover of the effective exponent η_{eff} for $N = 3$.

Borel transformation combined with conformal mapping and use of Padé approximants, it was shown that the fixed point governing the chiral critical behavior is a stable node only for large enough N, $N > N^*$. For smaller N a chiral fixed point turns out be a stable focus and the RG trajectories approach this point in a spiral-like manner. Of particular importance is the fact that a focus-driven critical behavior was found for systems with physical values of N, $N = 2, 3$. Evaluating the critical exponent η along some RG trajectories, we demonstrate that spiral-like approach of the chiral fixed point results in unusual crossover and near-critical regimes that may imitate varying critical exponents seen in physical and computer experiments.

ACKNOWLEDGMENTS

We would like to thank Ettore Vicari for many useful discussions. The financial support of the Russian Foundation for Basic Research under Grant No. 01-02-17048 (E.V.O., A.I.S.) and the Ministry of Education of Russian Federation under Grant No. E00-3.2-132 (E.V.O., A.I.S.) is gratefully acknowledged. A.I.S. has benefited from the warm hospitality of Scuola Normale Superiore and Dipartimento di Fisica dell'Università di Pisa, where the major part of this research was done.

REFERENCES

[1] H. Kawamura, Phys. Rev. B **38**, 4916 (1988); erratum B **42**, 2610 (1990).
[2] H. Kawamura, J. Phys.: Condens. Matter **10**, 4707 (1998).
[3] A. Pelissetto and E. Vicari, Phys. Rep. **368**, 549 (2002).
[4] P. Calabrese and P. Parruccini, Phys. Rev. B **64**, 184408 (2001).
[5] H. J. Luo, L. Schülke, and B. Zheng, Phys. Rev. Lett. **81**, 180 (1998); Phys. Rev. E **57**, 1327 (1998).
[6] R. Melzi, P. Carretta, A. Lascialfari, M. Mambrini, M. Troyer, P. Millet, and F. Mila, Phys. Rev. Lett. **85**, 1318 (2000); R. Melzi, S. Aldorovandi, F. Tedoldi, P. Carretta, P. Millet, and F. Mila, Phys. Rev. B **64**, 024409 (2001); P. Carretta, R. Melzi, N. Papinutto, and P. Millet, Phys. Rev. Lett. **88**, 047601 (2002).
[7] Q.-H. Chen, M.-B. Luo, and Z.-K. Jiao, Phys. Rev. B **64**, 212403 (2001).
[8] S. Faßbender, M. Enderle, K. Knorr, J. D. Noh, and H. Rieger, Phys. Rev. B **65**, 165411 (2002); M. Enderle, K. Knorr, J. D. Noh, and H. Rieger, Phys. Rev. E **66**, 026111 (2002).
[9] S. A. Antonenko, A. I. Sokolov and K. B. Varnashev, Phys. Lett. A **208**, 161 (1995).
[10] A. Pelissetto, P. Rossi and E. Vicari, Nucl. Phys. B **607**, 605 (2001).
[11] S. A. Antonenko and A. I. Sokolov, Phys. Rev. B **49**, 15901 (1994).
[12] M. Tissier, B. Delamotte, and D. Mouhanna, Phys. Rev. Lett. **84**, 5208 (2000); cond-mat/0107183.
[13] A. Pelissetto, P. Rossi, and E. Vicari, Phys. Rev. B **63** 140414(R) (2001), *ibid.* **65** 020409(R) (2002).
[14] P. Calabrese, P. Parruccini, and A. I. Sokolov, e-print cond-mat/0205046, Phys. Rev. B to appear.
[15] P. Calabrese, P. Parruccini, and A. I. Sokolov, in preparation.
[16] G. Parisi, Cargèse Lectures (1973) (unpublished); J. Stat. Phys. **23**, 49 (1980).
[17] J. Zinn-Justin, *Quantum Field Theory and Critical Phenomena*, third edition (Clarendon Press, Oxford, 1996).
[18] P. Calabrese, M. Caselle, A. Celi, A. Pelissetto, and E. Vicari, J. Phys A **33**, 8155 (2000).
[19] E. V. Orlov and A. I. Sokolov, Fiz. Tverd. Tela **42**, 2087 (2000) [Phys. Sol. State **42**, 2151 (2000)].
[20] Note that due to a misprint, the coefficient $b_{2,1}^{(u)} R_{2N}^{-3}$ in Tab. III of Ref. [4] should be read $-0.276622342 + \ldots$, instead of $+0.276622342 + \ldots$.
[21] J. C. Le Guillou and J. Zinn-Justin, Phys. Rev. Lett. **39**, 95 (1977); Phys. Rev. B **21**, 3976 (1980).
[22] J.M. Carmona, A. Pelissetto, and E. Vicari, Phys. Rev. B **61**, 15136 (2000).
[23] E. Brézin, J. C. Le Guillou, and J. Zinn-Justin, Phys. Rev. D **15**, 1544, 1588 (1977).
[24] B. G. Nickel, Phase Transitions ed. M. Lévy, J. C. Le Guillon and J. Zinn Justin (New York: Plenum), p. 291 (1982); Physica A **117**, 189 (1991).
[25] A. Pelissetto and E. Vicari, Nucl. Phys. B **519**, 626 (1998).
[26] T. Dombre and N. Read, Phys. Rev. B **39**, 6797 (1989); P. Azaria, B. Delamotte, and T. Jolicoeur, Phys. Rev. Lett. **64**, 3175 (1990); H. Kawamura, J. Phys. Soc. Jpn. **60**, 1839 (1991); P. Azaria, B. Delamotte, F. Delduc, and T. Jolicoeur, Nucl. Phys. B **408**, 485 (1993).

[27] D. Loison, A. I. Sokolov, B. Delamotte, S. A. Antonenko, K. D. Schotte, and H. T. Diep, Pis'ma v Zh.E.T.F. **72**, 487 (2000) [JETP Letters **72**, 337 (2000)].
[28] A. L. Korzhenevskii and B. N. Shalaev, Zh. Eksp. Teor. Fiz. **76**, 2166 (1979) [Sov. Phys. JEPT **49**, 1094 (1979)].
[29] A. I. Sokolov, Zh. Eksp. Teor. Fiz. **77**, 1598 (1979) [Sov. Phys. JEPT **50**, 802 (1979)].
[30] Y. Meurice, G. Ordaz, and V. G. J. Rodgers, Phys. Rev. Lett. **75**, 4555 (1995).